

JOURNAL OF SCIENCE



SAKARYA UNIVERSITY

Sakarya University Journal of Science

ISSN 1301-4048 | e-ISSN 2147-835X | Period Bimonthly | Founded: 1997 | Publisher Sakarya University |
<http://www.saujs.sakarya.edu.tr/>

Title: Effects of uniform radial electric field on the MHD and heat transfer due to a shrinking/stretching rotating disk

Authors: Nihan Uygun Ercan

Received: 2018-10-01 00:00:00

Accepted: 2019-02-04 00:00:00

Article Type: Research Article

Volume: 23

Issue: 4

Month: August

Year: 2019

Pages: 588-599

How to cite

Nihan Uygun Ercan; (2019), Effects of uniform radial electric field on the MHD and heat transfer due to a shrinking/stretching rotating disk. Sakarya University Journal of Science, 23(4), 588-599, DOI: 10.16984/saufenbilder.466151

Access link

<http://www.saujs.sakarya.edu.tr/issue/43328/466151>

New submission to SAUJS

<http://dergipark.gov.tr/journal/1115/submission/start>

Effects of uniform radial electric field on the MHD and heat transfer due to a shrinking/stretching rotating disk

Nihan Uygun*¹

Abstract

Flow and heat transfer of an incompressible electrically conducting fluid on radially shrinking/stretching rotating disk in presence of uniform magnetic field are studied in the present paper. The problem is an extension of the well-known von Karman viscous pump problem to the configuration with a shrinkable/stretchable disk with or without rotation. Navier-Stokes equations, Maxwell equation and energy equation have been modified in presence of uniform radial electric field and magnetic field. The governing partial differential equations have been transformed into ordinary differential form by using similarity transformations. The system of equations generated by Navier-Stokes, Maxwell and energy equations has been solved by using Chebyshev collocation technique for varying values of radial electric, magnetic interaction parameters, Eckert and rotation numbers. Accuracy of the method is verified through comparing results in the literature. Effects of parameters in the governing equations are depicted graphically and are analyzed.

Key Words: Electric potential, Radial shrinking, Radial stretching, MHD flow.

1. INTRODUCTION

Boundary layer flow due to rotating disk has been received substantial interest. In particular, MHD fluid flow and heat transfer have been examined in many recent researches. In the last few decades, some problems which are interesting from both engineering and mathematical points of view have been investigated. The rotating disk flows of MHD fluids are not only of theoretical interest, but they are also of considerable practical significance. Fluid flow due to shrinkable/stretchable disk are important in many applications such as glass fiber and paper production, cooling of metallic sheets or electronic chips, hot rolling, thermal-power generating systems, rotating machinery, medical equipments, computer storage devices, gas turbine rotors, air cleaning machines, aerodynamical applications, crystal growth process,

extrusion process in plastic and metal industries. In this paper, radial electric field is explored for the MHD fluid flow and heat transfer over shrinking/stretching rotating disk.

Pioneering study of fluid flow was carried out by Von Karman[13], thus many explanations are initiated on infinite rotating disk. Basing on the work of Karman[13], Cochran[4] and Benton[3] investigated steady motion of an incompressible viscous fluid as a means of numerical and asymptotical forms. Crane[6] obtained a similarity solution in closed analytical form for steady two dimensional incompressible boundary layer flow caused by stretching of a sheet. Papers of Altan, Oh& Gegel[1], Fisher[11] and [19], the flow induced by a moving boundary, are important in the extrusion processes in plastic and metal industries. Stretching boundary problem was extended to a three-dimensional case by Wang[25]. Fang[8] obtained an

* Corresponding Author

¹ Bolu Abant İzzet Baysal Üniversitesi, Fen Edebiyat Fakültesi, Matematik Bölümü, 14030 BOLU, nuygun@ibu.edu.tr

exact solution for the steady state Navier-Stokes equation in cylindrical coordinates. Fang and Zhang studied the flow between two stretching disks in [10]. Watson and Wang[29] studied the unsteady flow over a rotating disk. Shrinking problems can also be applied to the study of capillary effects in small pores and the hydraulic properties of agricultural clay soils. Studies of flow due to a shrinking sheet have been considered by Makukula[15], among others,[2], [5], [9], [16], [28].

Effect of the uniform magnetic field on the flow over a rotating infinite disk has been studied by many researchers in [18], [20], [21], [22], [23], [24]. Effects of the uniform radial electric field on the MHD heat and fluid flow due to a rotating disk was investigated by Turkyilmazoglu[20]. Effects of the radial electric field have been taken into consideration in some works in the literature [20], [24]. To our best knowledge, Turkyilmazoglu[20] has initiated in his studies examining effects of radial electric field on the flow over a infinite rotating disk. Following that work, Uygun[24] studied analysis of Hall current due to a rotating disk with uniform radial electric field.

Heat transfer problem on the shrinking/stretching rotating disk has been studied by Turkyilmazoglu in [22], [23]. In his works, results of behavior of the flow and temperature fields on shrinking disk and stretching disk effects have been investigated and compared.

In the literature, most of the studies in rotating disk neglected the induced electric field yielding a Lorentz force density free of the electric field. In this case the term of Lorentz force density free of the electrical field would not be properly correct, without vorticity of the flow which is perpendicular to the magnetic field in the entire domain. Since all three velocity components are nonzero in the flow, above assumption may not be possible. Therefore, the electric field is important and it has a significant effect on the Lorentz force term.

In the present work, the steady hydromagnetic flow of viscous, incompressible fluids over shrinking/stretching disk is examined with induced uniform electric field in the radial direction. This problem is an extension of well-known von Karman viscous pump problem to the configuration with a shrinkable/stretchable disk with or without rotation. In this work, an external uniform magnetic field is imposed in the wall normal direction, and a radial electric field produced by electric potential is applied. Because of the existence of uniform radial electric

field at the infinity, a radial pressure gradient is generated. In the disk flow, the magnetic Reynolds number is assumed to be very small. Navier-Stokes equations, Maxwell equation and the energy equation have been modified for taken into account the presence of uniform radial electric field and magnetic field. The governing partial differential equations have been transformed into the form of non-linear ordinary differential equations by using Karman's similarity transformations. The system of equations generated by Navier-Stokes, Maxwell and energy equations has been solved using spectral Chebyshev collocation technique for varying values of radial electric, magnetic interaction, rotation parameters, and Eckert number. The effects of uniform electric field in the radial direction on the shrinking/stretching disk flow is analyzed.

2. MATHEMATICAL ANALYSIS

We consider the three-dimensional steady viscous incompressible electrically conducting fluid occupying a semi infinite region over a rigid disk rotating about its axis with a constant angular velocity Ω in the cylindrical coordinate (r, θ, z) . The terminology given for an external uniform magnetic field and electric field in Turkyilmazoglu[22] and Uygun[24] is followed. The disk flow motion is governed by Maxwell's equation, continuity equation, Navier-Stokes equations including the Lorentz force and energy equation with viscous dissipation and Joule heating are as follows,

$$\nabla \cdot \mathbf{j} = 0 \quad (1)$$

$$\nabla \cdot \mathbf{v} = 0 \quad (2)$$

$$\rho \left[\frac{\partial \mathbf{v}}{\partial t} + (\mathbf{v} \cdot \nabla) \mathbf{v} \right] = -\nabla p + \frac{1}{Re} [\nabla^2 \mathbf{v}] + M_n (\mathbf{j} \times \mathbf{B})_i \quad (3)$$

$$\rho \left[\frac{\partial T}{\partial t} + (\mathbf{v} \cdot \nabla) T \right] = M_\infty^2 (\Gamma - 1) \left[\frac{\partial p}{\partial t} + (\mathbf{v} \cdot \nabla) p \right] + \frac{1}{Pr} \frac{1}{Re} [\nabla^2 T] + \frac{\Gamma - 1}{Re} M_\infty^2 [\Phi] + M_n (\Gamma - 1) M_\infty^2 \frac{j^2}{\sigma} \quad (4)$$

Lorentz force terms $M_n (\mathbf{j} \times \mathbf{B})_i$ play an important role in fluid motion equations of magnetic field. This means that the velocity and pressure characteristics of the flow can be altered by the presence of the force on the flow of conducting fluids. On the other hand, due to radial electric field imposed to velocity at the infinity, the tangential direction velocity is given by $v = \Omega \gamma r$. Furthermore, existence of potential flow induced by radial electric field at the edge of the

boundary layer implies that pressure gradient in the radial direction is $\frac{\partial p}{\partial r} = \rho \Omega^2 \gamma^2 r$ (see Evans[7]).

The parameters in equations (1-4) are following: ρ the density, $\mathbf{v} = (u, v, w)$ the velocity vector, ∇ the usual gradient operator in cylindrical coordinates, p the pressure, Re is the Reynolds number characterizing the flow defined by $Re = \frac{s\Omega}{\nu}$, ν is the kinematic viscosity of the fluid, M_n is the magnetic interaction parameter which represents the ratio between the magnetic force to the fluid inertia force, T is the temperature of the fluid, $Pr = \frac{\mu c_p}{k}$ is the Prandtl number, c_p is the specific heat capacity, μ is the dynamical viscosity and k is thermal conductivity of the fluid. Finally, Γ is the ratio of the specific heats, M_∞ is the free stream Mach number.

The basic flow of incompressible case, also called as Von Karman's steady state flow, is well known. The Von Karman's [13] flow will be considered, which means that the disk flow is assumed to evolve alongside the boundary layer coordinate $\eta = Re^{1/2}z$, in conformity with the self similarity variables (see Hossain, Hossain & Wilson[12]),

$$\begin{aligned} (u, v, w) &= (rs\Omega F(\eta), rs\Omega G(\eta), Re^{-1/2}H(\eta)) \\ (p, T) &= (\rho\Omega^2 P(\eta), T_\infty + (T_w - T_\infty)\theta(\eta)) \\ (j_r, j_\theta, j_z) &= (B_0rs\Omega J_r(\eta), B_0rs\Omega J_\theta(\eta), B_0\Omega Re^{-1/2}J_z(\eta)) \\ (e_r, e_\theta, e_z) &= (B_0rs\Omega E_r(\eta), 0, B_0\Omega Re^{-1/2}E_z(\eta)) \end{aligned} \tag{5}$$

where T_w is the temperature at the surface of the disk, T_∞ is the temperature of the ambient fluid at far from the disk. These quantities in (5) inserted into the governing equations (1-4), and also neglect terms of $O(Re^{-1})$, then the disk flow quantities are determined from the subsequent equations,

$$2J_r + J_z' = 0, \tag{6}$$

$$2F + H' = 0, \tag{7}$$

$$F^2 - G^2 + F'H - F'' - M_n [-F] + \gamma^2 = 0, \tag{8}$$

$$2FG + G'H - G'' - M_n [\gamma - G] = 0, \tag{9}$$

$$P' + H'H - H'' = 0, \tag{10}$$

$$\begin{aligned} \frac{1}{Pr}\theta'' - H\theta' + E_c [\gamma^2 F + F^2 + G^2] + M_n E_c [(-\gamma + G)^2 \\ + (-F)^2] = 0 \end{aligned} \tag{11}$$

where $E_c = \frac{M_\infty^2(\Gamma - 1)}{T_w - T_\infty}$ is the Eckert number. A prime denotes derivative with respect to η . The initial and

boundary conditions appropriate to the shrinkable and stretchable disk flow are given respectively as,

$$F = -1, G = \omega, H = 0, J_z = 2C\gamma, \theta = 0, \text{ at } \eta = 0, \tag{12}$$

$$F \rightarrow 0, G \rightarrow \gamma, \theta \rightarrow 1, \text{ as } \eta \rightarrow \infty,$$

$$F = 1, G = \omega, H = 0, J_z = 2C\gamma, \theta = 0, \text{ at } \eta = 0, \tag{13}$$

$$F \rightarrow 0, G \rightarrow \gamma, \theta \rightarrow 1, \text{ as } \eta \rightarrow \infty,$$

where C is the wall conduction ratio of the electrical conductance of the wall to electrical conductivity of the fluid and $\omega = \Omega/s$ represents a rotation strength parameter measuring the ratio of swirl to shrink/stretch and $\omega = 0$ means a pure shrinking/stretching without rotation. We should denote that equations (6-11) and boundary condition (12) can be described as an extension of the problem of Fang[8] in the nonmagnetic and non-heat conducting flow case. It can be easily shown that integration of the third momentum equation implements the shrinking/stretching pressure.

The heat transfer from the disk surface to the fluid is computed by application of the Fourier's law and by using transformation for heat term we obtain

$$q = -k \left(\frac{\partial T}{\partial z} \right)_w = -k(T_w - T_\infty) \sqrt{\frac{s\Omega}{\nu}} \frac{d\theta(0)}{d\eta} \tag{14}$$

By rephrasing the heat transfer result, we can get the Nusselt number as $N_u = \frac{q \sqrt{\frac{\nu}{s\Omega}}}{k(T_w - T_\infty)}$.

The action of viscosity in the fluid adjacent to the disk tends to set up tangential shear stress, which opposes the rotation of the disk. Also, in the radial direction there is a surface shear stress. Applying the Newtonian formula, the radial τ_r and tangential components τ_θ of the shear stress are respectively expressed by

$$\tau_r = \left(\frac{\partial u}{\partial z} \right)_w = r\Omega \sqrt{\frac{s\Omega}{\nu}} F'(0) \tag{15}$$

$$\tau_\theta = \left(\frac{\partial v}{\partial z} \right)_w = r\Omega \sqrt{\frac{s\Omega}{\nu}} G'(0) \tag{16}$$

Of physical interest is also the magnitude of the constant axial velocity at infinity, given by $H(\infty)$.

In this work, we numerically solved the equations (6-11) under the shrinking boundary conditions (12) and the stretching boundary conditions (13) respectively by using Chebyshev collocation method which is a matrix method. This method transforms the differential integral equations to a matrix equation, which corresponds to a system of linear algebraic equations with unknown Chebyshev coefficients.

3. RESULTS AND DISCUSSIONS

In this section, we considered the system of differential equations (6-11) under the the shrinking boundary conditions (12) and the stretching boundary conditions (13), and through using these flow profiles, relevant calculations are made for the shrinking(12)/stretching(13) boundary conditions. The numerical results are obtained by utilizing Spectral Chebyshev collocation scheme basing on Chebyshev polynomials.

To verify the accuracy of the Chebyshev collocation method, we compared studies of Fang[8] and Turkyilmazoglu [23]. A comparison with the results of Fang [8] for stretchable disk, and Turkyilmazoglu [23] for shrinkable disk are tabulated in Table 1 and Table 2, respectively. These tables give a clear evidence for the accuracy of the numerical method. Moreover, figures 1(a)-1(b) which shows the velocity profiles of the shrinking/stretching boundary layer flow over the rotating disk are in confirmety with the graphs given in Fang[8] and Turkyilmazoglu [23].

M_n	$F'(0)$	
0.0	Present	Fang
	-1.1737208820308371	-1.173721

Table 1: Comparison of the numerical solutions of the radial shear stress coefficient, $F'(0)$ over stretchable disk.

We solved the equations (6-11) both under the shrinking(12) and stretching(13) conditions to compute various velocity and temperature profiles as depicted in Figures (2-11). These graphs show effects of the radial electric parameters, magnetic interaction parameters, rotation parameters and Eckert numbers in governing equations over shrinking/stretching disk.

M_n	ω	Present	Türkyilmazoglu
$F'(0)$			
0.0	0.0	-0.72513189	-0.725131902
	5.0	7.823330854	7.823330854

2.0	5.0	6.776728181	6.776728182
$H(\infty)$			
0.0	0.0	-0.940908420	-0.940971451
	5.0	1.784926562	-1.784926562
2.0	5.0	-0.703176935	-0.703176935
$-\theta'(0)$			
0.0	0.0	-6.06951E-008	0.000000001
	5.0	0.646260815	0.646260815
2.0	5.0	0.363763399	0.363763019

Table 2: Comparison of numerical solutions of the radial shear stress coefficient, $F'(0)$, the vertical velocity, $H(\infty)$ and the coefficient of the heat transfer, $-\theta'(0)$ over shrinkable disk.

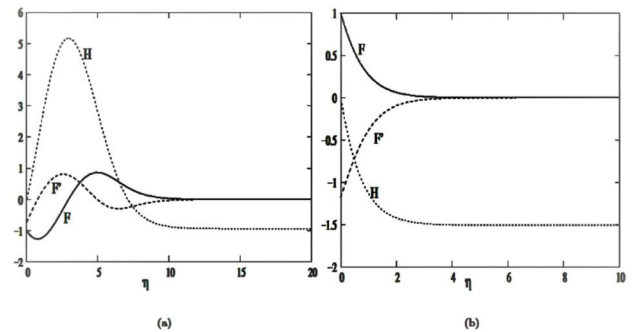


Figure 1: Velocity profiles of the shrinkable/stretchable disk flow are shown against the coordinate η , respectively in (a) shrinking disk, (b) stretching disk.

It can be inferred from these pictures that regardless having the radial electric parameter γ positive or negative values, the radial velocity profile near the disk increases as the rotation parameter increases. This situation occurs as a result of the fluid particles in the radial direction pushed by centrifugal force, while rotation parameter increases. However far away from the disk reverse effect takes place. This means that the effects of the centrifugal force is restricted to the vicinity of the disk surface. Although this feature of the radial velocity is valid for all its positive and negative values, there is an impressive increment on the radial component of velocity near the shrinking disk in the case of positive radial electric parameter.

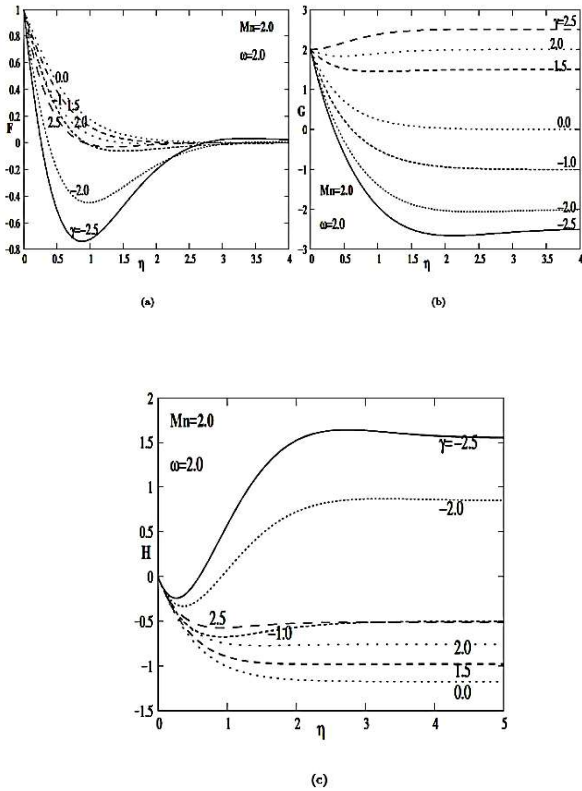


Figure 2: Velocity profiles of the generalized Von Karman's flow are shown for $M_n = 2.0$ and $\omega = 2.0$ at the six different radial electric parameters, respectively in (a) for radial F , (b) for tangential G , (c) for axial H components over stretchable disk.

In stretching disk, these current cases are similar with the cases in shrinking disk. In addition, for both the shrinking disk in figures (5(a)-7(a)) and the stretching disk in figures (2(a)-4(a)), the size of the interval of η shrinks as the rotation parameter increases. Moreover, where the radial electric parameter is positive, any increment in the value of a Magnetic interaction parameter has no significant effect on the radial velocity profile. On the other hand, when the radial electric parameter takes negative value, the radial component of the velocity profiles increases while a Magnetic interaction parameter increases over stretching disk as given in figures (2(a)-4(a)).

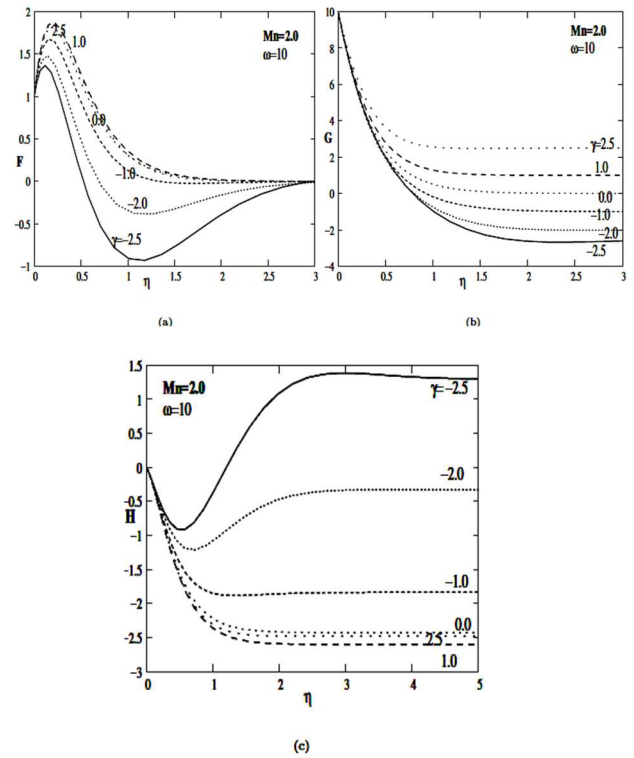


Figure 3: Velocity profiles of the generalized Von Karman's flow are shown for $M_n = 2.0$ and $\omega = 10.0$ at six different radial electric parameters, respectively in (a) for radial F , (b) for tangential G , (c) for axial H components over stretchable disk.

In the shrinking disk, not only the radial electric parameters take positive values, but also the radial electric parameters take negative values, it is also apparent similar effect with stretching disk as a Magnetic interaction parameter increases from graphs (5(a)-7(a)). All of these can be easily seen in tables(3-4).

Graphs (2(b)-7(b)) illustrates influence of radial electric parameter on the tangential velocity profile. When the radial electric parameter increases, the tangential velocity increases both in shrinking and stretching disks. Near the wall of shrinking disk it more increases than near the wall of stretching disk for positive radial electric parameter as the rotation parameter gets small values. Moreover, it can be visualized from these pictures that the tangential velocity profile increases as the magnetic interaction parameter increases for positive radial electric parameter. On the other hand, when the radial electric parameter becomes negative, the change of the tangential velocity profile is not significant as the

magnetic interaction parameter increases or decreases. The last two cases in the shrinking disk is similar to the case in the stretching disk.

and rotation number in the shrinking disk. All the cases on axial velocity profiles in shrinking disk like as the cases in the stretching disk. All of these can be clearly seen in tables (3-4).

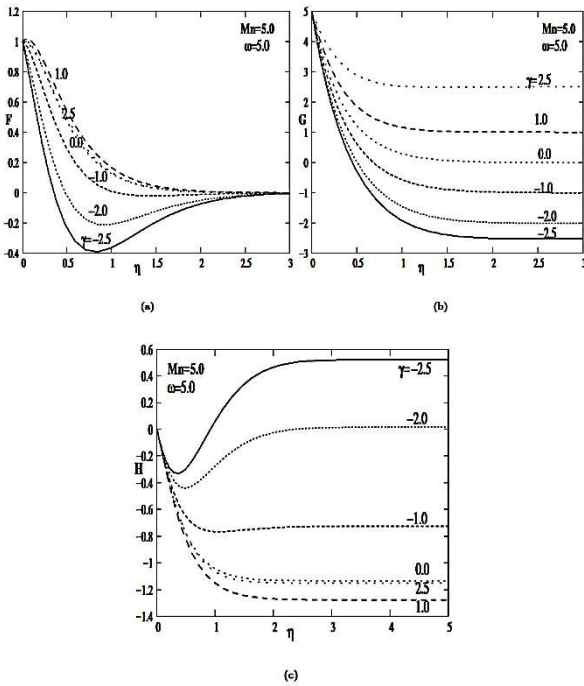


Figure 4: Velocity profiles of the generalized Von Karman are shown for $M_n = 5.0$ and $\omega = 5.0$ at six different radial electric parameters, respectively in (a) for radial F , (b) for tangential G , (c) for axial H components over stretchable disk.

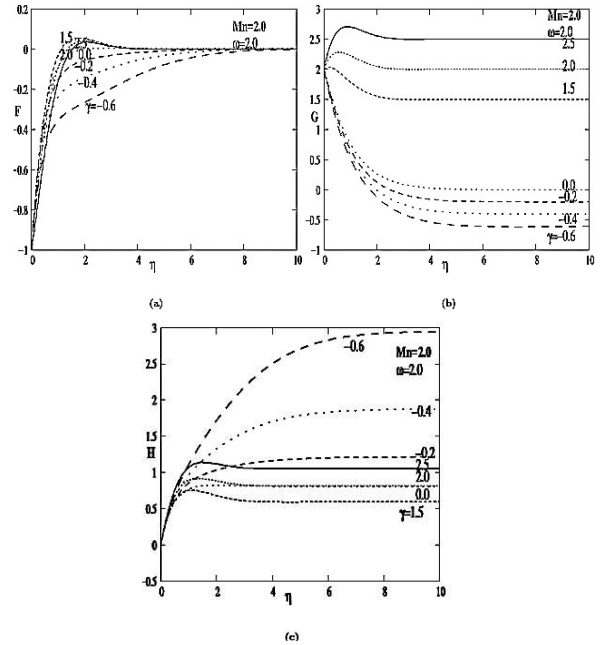


Figure 5: Velocity profiles of the generalized Von Karman are shown for $M_n = 2.0$ and $\omega = 2.0$ at six different radial electric parameters, respectively in (a) for radial F , (b) for tangential G , (c) for axial H components over shrinkable disk.

For the stretching disk, effects of the radial electric parameter in the axial component of the velocity can be visualized in figures (2(c)-4(c)). It can be inferred from these graphs that positive radial electric parameter has a big impact on the axial velocity profiles. In case of having the radial electric parameter negative, it does not cause to a significant change in the axial velocity profile as the rotation parameter increases. However, while the radial electric parameter takes positive value the axial component of the velocity profiles decreases as the rotation parameter increases in the stretching disk. Meanwhile, when the radial electric parameter takes negative values the axial velocity decreases, in case of positive radial electric parameter the change of velocity on axial component is not important as the magnetic interaction number becomes stronger in the stretching disk. Graphs (5(c)-7(c)) show effects of the radial electric parameter, Magnetic interaction parameter

Figures (8-11) demonstrate temperature profiles which depend on the velocity components for different electric parameters in radial direction, Eckert numbers, Magnetic interaction numbers and rotation parameters at the fixed Prandtl number $P_r = 1.0$. Effects of the radial electric parameter depicted in graphs (8-11). It can be obviously inferred from these pictures that negative radial electric parameter has an influence on temperature profiles for shrinking and stretching disks.

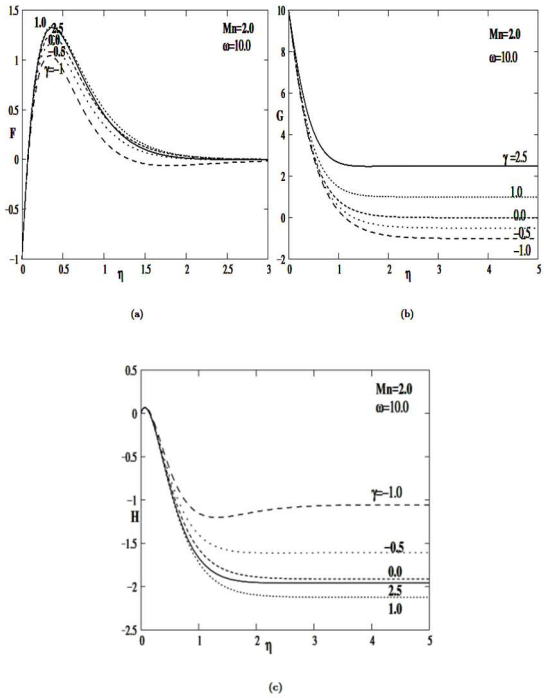


Figure 6: Velocity profiles of the generalized Von Karman are shown for $M_n = 2.0$ and $\omega = 10.0$ at six different radial electric parameters, respectively in (a) for radial F , (b) for tangential G , (c) for axial H components over shrinkable disk.

For the shrinking disk, when the rotational number increases size of interval of η shrinks. Conversely for the stretching disk the effect of increasing rotational number becomes reversed. On the other hand, not only in shrinking disk but also in stretching disk, size of interval η extends as the Magnetic interaction number increases for all values of radial electric parameters.

Furthermore, whenever rotation parameter increases more, temperature profile is likely to be present for negative radial electric parameters. The case can be seen in figures (8) and (11). This means that the number of presence of temperature profiles increases for negative radial electric parameters as rotation parameter increases in both shrinking and stretching cases.

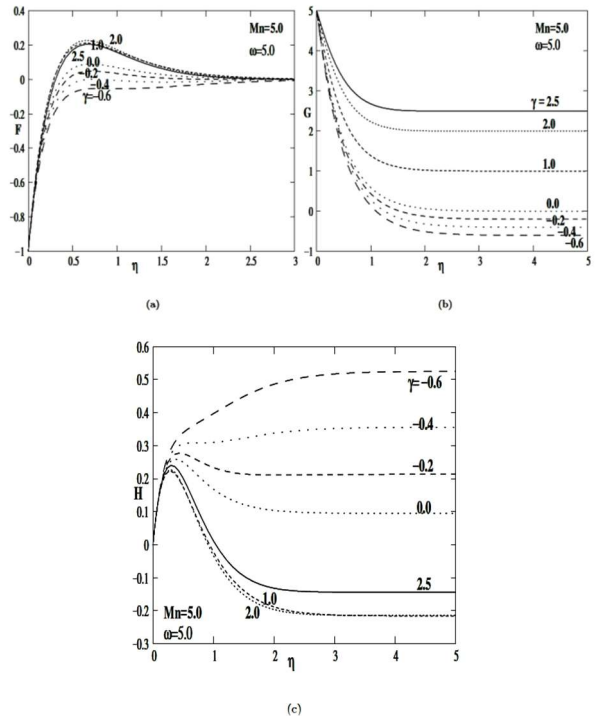


Figure 7: Velocity profiles of generalized Von Karman are shown for $M_n = 5.0$ and $\omega = 5.0$ at six different radial electric parameters, respectively in (a) for F radial, (b) for G tangential, (c) for H axial components over shrinkable disk.

It is also apparent from graphs (9) that when positive Eckert number increases, temperature profile increases in shrinking disk. Finally, decline in the radial parameter causes an increment in the temperature profiles in shrinking disk. These two cases provide similar features for stretching disk. It can be clearly seen in graph (8).

Variations of the radial shear stress $F'(0)$, tangential shear stress $G'(0)$, the velocity in the radial direction $H(\infty)$ and coefficients of heat transfer $-\theta'(0)$ have been tabulated with various radial electric parameter γ for two different magnetic interaction numbers $M_n = 1.0$, $M_n = 3.0$, and for three different Eckert numbers $E_c = -3.0$, $E_c = 0.0$ and $E_c = 3.0$ respectively in tables (3-6).

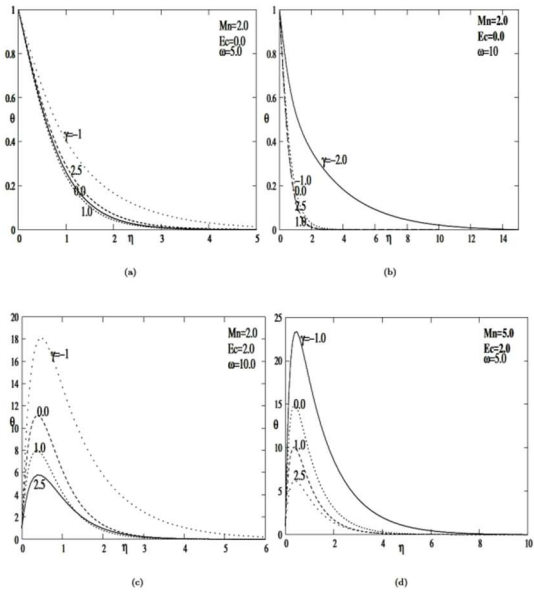


Figure 8: Temperature profile corresponding to heat transfer case is shown at different radial electric parameters respectively in (a) for $M_n=2.0$, $E_c=0.0$ and $\omega=5.0$ (b) for $M_n=2.0$, $E_c=0.0$ and $\omega=10.0$, (c) for $M_n=2.0$, $E_c=2.0$ and $\omega=10.0$, (d) for $M_n=5.0$, $E_c=2.0$ and $\omega=5.0$, over stretchable disk.

When negative radial electric parameter increases the radial shear stress decreases for negative Eckert numbers. Its reverse effect is apparent when the radial electric parameter becomes positive in shrinking disk. These cases in shrinking radial shear stress are similar to the cases in stretching disk. It can be clearly seen in tables (3-4). It is also inferred from these tables because of increasing the rotation parameter initially for negative radial electric parameter, and then for all values of radial electric parameter, characteristic of the radial shear stress is changed as the Magnetic interaction number increases in shrinking disk. On the other hand, in stretching disk the radial shear stress decreases, except for beginning of rotation at enough large radial electric parameters as the Magnetic interaction parameter increases.

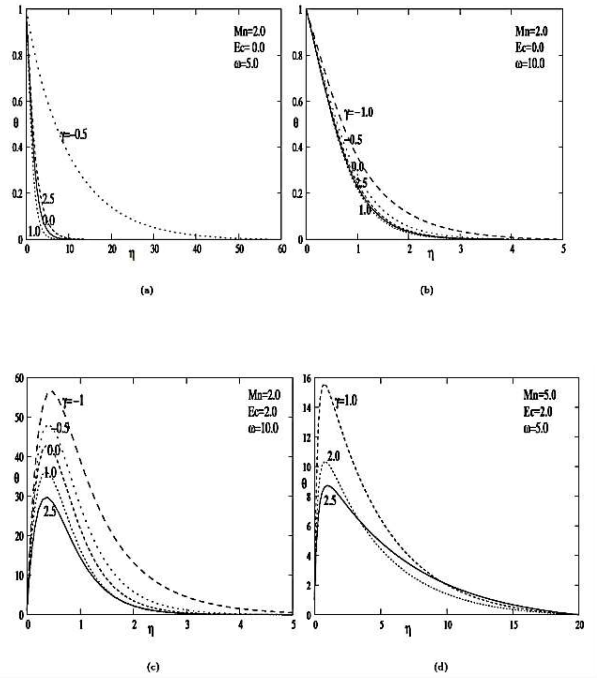


Figure 9: Temperature profile corresponding to heat transfer case is shown at different radial electric parameters respectively in (a) for $M_n=2.0$, $E_c=0.0$ and $\omega=5.0$, (b) for $M_n=2.0$, $E_c=0.0$ and $\omega=10.0$, (c) for $M_n=2.0$, $E_c=2.0$ and $\omega=10.0$, (d) for $M_n=5.0$, $E_c=2.0$ and $\omega=5.0$, over shrinkable disk.

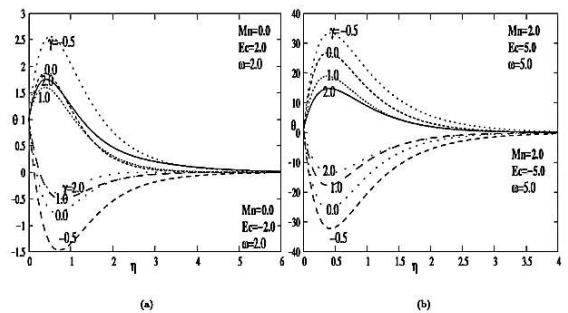


Figure 10: Temperature profile corresponding to heat transfer case is shown at different radial electric parameters respectively in (a) $M_n=0.0$, and $\omega=2.0$ for two different Eckert numbers $E_c=2.0$ and $E_c=-2.0$, (b) $M_n=2.0$, and $\omega=5.0$ for two different Eckert numbers $E_c=5.0$ and $E_c=-5.0$ over stretchable disk.

When the magnetic interaction parameter M_n increases, behavior of the tangential shear stress in shrinking disk and in stretching disk becomes similar. That is, the tangential shear stress decreases as the radial electric parameter becomes negative, tangential

shear stress increases when radial electric parameter gets positive value at the beginning of the rotation. When the rotation speed up, shear stress in the tangential direction only decreases. In the two cases, negative radial electric parameter has a big impact on the tangential shear stress.

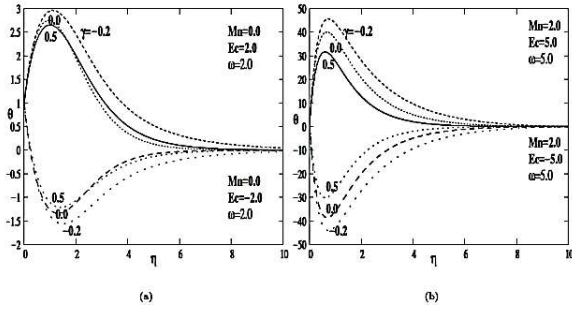


Figure 11: Temperature profile corresponding to heat transfer case is shown at different radial electric parameters respectively in (a) $M_n = 0.0$, and $\omega = 2.0$ for two different Eckert numbers $E_c = 2.0$ and $E_c = -2.0$, (b) $M_n = 2.0$, and $\omega = 5.0$ for two different Eckert numbers $E_c = 5.0$ and $E_c = -5.0$ over shrinkable disk.

Finally, the impacts of radial electric parameters in coefficients of heat transfer can be deduced from tables (5-6). These tables show that when Eckert number becomes negative the heat transfer coefficients decreases for negative radial electric parameter. On the other hand, if the radial electric parameter is positive, the effect on the coefficients of heat transfer becomes reversed. Moreover, in shrinking disk while the rotation parameter increases, coefficients of heat transfer increase until the radial electric parameter larger than unity. In case of stretching disk the effect reversed for all values of radial electric parameters. In these cases Eckert number is negative. Above mentioned situation is still valid for increment of the magnetic interaction parameter. Furthermore, it can be deduced from tables (5-6) that heat transfer coefficients decrease for all values of the radial electric parameters as Eckert number increases both in shrinking and in stretching disk.

M_n	ω	γ	$F'(0)$	$G'(0)$	$H(\infty)$
1.0	0.0	-0.6	-0.15330	-0.85845	5.2583
		-0.4	-5.92E-002	-0.57681	9.40263
		0.0	3.98E-008	2.14E-013	19.89864
		0.3	-3.01E-002	0.43581	12.51627
		0.9	-0.37952	1.29442	3.08307
		1.5	-1.08216	2.25349	2.93132
		2.5	-2.79846	4.13338	3.06747
	2.0	-0.6	1.95551	-0.89422	5.15273
		-0.4	2.12276	-0.89286	1.93020
		0.0	2.34146	-0.77008	0.11841
		0.3	2.39951	-0.58721	-0.11906
		0.9	2.26573	-3.95E-002	5.68E-002
		1.5	1.84496	0.70270	0.42080
		2.5	0.62346	2.28634	1.01874
5.0	-0.6	6.91202	-5.47360	-0.21839	
	-0.4	7.04890	-5.48104	-0.71588	
	0.0	7.24465	-5.38649	-1.19930	
	0.3	7.32140	-5.23700	-1.32846	
	0.9	7.30072	-4.77424	-1.31054	
	1.5	7.06290	-4.12889	-1.12307	
	2.5	6.23272	-2.71875	-0.68486	

(a)

M_n	ω	γ	$F'(0)$	$G'(0)$	$H(\infty)$
1.0	0.0	-0.6	-1.71910	-0.65426	-1.00018
		-0.4	-1.61775	-0.43137	-1.113784
		0.0	-1.53571	2.27E-013	-1.21105
		0.3	-1.58197	0.32224	-1.15559
		0.9	-1.94258	1.00455	-0.77200
		1.5	-2.62251	1.78332	-0.21838
		2.5	-4.32183	3.35838	0.66328
	2.0	-0.6	-1.15040	-4.15924	-0.90739
		-0.4	-0.98821	-3.99541	-1.13539
		0.0	-0.79678	-3.63741	-1.39115
		0.3	-0.75838	-3.33819	-1.44423
		0.9	-0.91731	-2.65333	-1.32404
		1.5	-1.34877	-1.85024	-1.04435
		2.5	-2.57349	-0.25428	-0.46914
	5.0	-0.6	2.09399	-10.55055	-1.45819
		-0.4	2.26276	-10.45788	-1.66339
		0.0	2.49640	-10.20107	-1.91177
		0.3	2.58907	-9.95462	-1.99768
		0.9	2.58501	-9.34313	-2.00652
		1.5	2.35439	-8.59238	-1.88361
		2.5	1.52886	-7.07030	-1.53688

(b)

Table 3: Shear stress coefficients $F'(0)$ and $G'(0)$, vertical velocity $H(\infty)$ are tabulated at some rotation numbers, radial electric parameters for fixed Magnetic interaction number $M_n = 1.0$ over (a) shrinkable and (b) stretchable disk

M_n	ω	γ	$F'(0)$	$G'(0)$	$H(\infty)$
3.0	0.0	-0.6	1.15203	-1.06929	1.82013
		-0.4	1.23527	-0.71008	1.74756
		0.0	1.30234	2.42E-013	1.68477
		0.3	1.26456	0.53182	1.72064
		0.9	0.96703	1.61758	1.96340
		1.5	0.39398	2.76309	2.29821
		2.5	-1.08388	4.86205	2.80265
	2.0	-0.6	1.90758	-3.24647	1.89697
		-0.4	2.09199	-2.96221	1.49233
		0.0	2.34526	-2.37207	0.95179
		0.3	2.44121	-1.90797	0.73096
		0.9	2.41473	-0.91800	0.59615
		1.5	2.12754	0.16001	0.69144
		2.5	1.14946	2.15959	1.04923
	5.0	-0.6	5.93452	-8.32381	0.33614
		-0.4	6.12672	-8.13322	5.17E-002
		0.0	6.42012	-7.69733	-0.33009
		0.3	6.56504	-7.32719	-0.49790
		0.9	6.67637	-6.48780	-0.63645
		1.5	6.56879	-5.52876	-0.61147
		2.5	5.95385	-3.69168	-0.38448

(a)

M_n	ω	γ	$F'(0)$	$G'(0)$	$H(\infty)$
3.0	0.0	-0.6	-2.21047	-1.05563	-0.84494
		-0.4	-2.14076	-0.70218	-0.88773
		0.0	-2.08484	2.66E-013	-0.92260
		0.3	-2.11631	0.52622	-0.90291
		0.9	-2.36651	1.59130	-0.751806
		1.5	-2.85891	2.69271	-0.47970
		2.5	-4.17781	4.65951	0.12100
	2.0	-0.6	-1.77816	-5.55032	-0.81291
		-0.4	-1.65418	-5.22033	-0.90414
		0.0	-1.49295	-4.55301	-1.02656
		0.3	-1.44595	-4.04292	-1.06886
		0.9	-1.53341	-2.98826	-1.04458
		1.5	-1.84853	-1.87634	-0.90881
		2.5	-2.83317	0.12816	-0.53498
	5.0	-0.6	0.94701	-12.89744	-1.13171
		-0.4	1.11610	-12.62700	-1.25343
		0.0	1.37023	-12.05728	-1.42970
		0.3	1.49097	-11.60486	-1.51177
		0.9	1.56483	-10.63590	-1.57470
		1.5	1.43100	-9.58237	-1.53692
		2.5	0.78940	-7.64212	-1.33174

(b)

Table 4: Shear stress coefficients $F'(0)$ and $G'(0)$, vertical velocity $H(\infty)$ are tabulated at some chosen rotation numbers, radial electric parameters for fixed Magnetic interaction number $M_n = 3.0$ over (a) shrinkable and (b) stretchable disk.

M_n	E_c	ω	$\gamma = -0.6$	$\gamma = -0.4$	$\gamma = 0.0$	$\gamma = 0.3$	$\gamma = 1.5$	$\gamma = 2.5$
1.0	-3.0	0.0	3.165618	2.87580	2.65873	2.77852	6.41765	15.12368
		2.0	19.38806	17.87017	14.64714	12.16076	3.31717	-2.85497
		5.0	101.66715	93.33804	84.45677	78.97283	58.03975	40.05768
	0.0	0.0	4.55E-014	-1.44E-012	8.27E-008	9.55E-011	5.95E-014	6.78E-014
		2.0	1.32E-012	2.20E-006	1.86E-002	4.75E-002	4.30E-003	4.43E-005
		5.0	0.28113	0.42093	0.51177	0.53858	0.51327	0.38328
	3.0	0.0	-3.16561	-2.87580	-2.65873	-2.77852	-6.41765	-15.12368
		2.0	-19.38806	-17.87016	-14.60975	-12.06567	-3.30856	2.85506
		5.0	-101.10489	-92.49616	-83.43322	-77.89566	-57.01319	-39.29111
3.0	-3.0	0.0	5.77788	5.14523	4.63632	4.92292	11.68145	24.40944
		2.0	35.72379	31.64395	24.09805	19.04384	4.51372	-1.14287
		5.0	165.35940	154.12167	131.66025	117.68908	74.78612	46.59054
	0.0	0.0	1.13E-007	2.11E-007	3.59E-007	2.66E-007	1.47E-009	1.02E-011
		2.0	1.01E-007	2.14E-006	1.16E-004	5.72E-004	7.36E-004	4.13E-005
		5.0	1.72E-002	7.20E-002	0.21644	0.28382	0.33842	0.24810
	3.0	0.0	-5.77788	-5.14523	-4.63632	-4.92292	-11.68145	-24.40944
		2.0	-35.72379	-31.64395	-24.09781	-19.04269	-4.51225	1.14296
		5.0	-165.32487	-153.97764	-131.22737	-117.12142	-74.10927	-46.09433

Table 5: Heat transfer parameter $-\theta'(0)$ is tabulated at some chosen rotation numbers, $\omega = 0.0, 2.0, 5.0$, radial electric parameters, $\gamma = -0.6, -0.4, 0.0, 0.3, 1.5, 2.5$, for the two different Magnetic interaction numbers $M_n = 1.0, 3.0$, and Eckert numbers $E_c = -3.0, 0.0, 3.0$ respectively, and fixed Prandtl number $P_r = 1.0$ over shrinkable disk.

M_n	E_c	ω	$\gamma = -0.6$	$\gamma = -0.4$	$\gamma = 0.0$	$\gamma = 0.3$	$\gamma = 1.5$	$\gamma = 2.5$
1.0	-3.0	0.0	5.30157	4.39098	3.65634	4.07031	13.68861	29.61070
		2.0	24.10858	20.80647	15.77202	13.02879	8.48988	10.56952
		5.0	104.19927	98.47357	88.46170	81.79152	59.87636	46.06093
	0.0	0.0	0.72628	0.75728	0.78093	0.76775	0.32986	2.20E-003
		2.0	0.73284	0.79257	0.85031	0.86289	0.75419	0.46796
		5.0	0.96893	1.00685	1.05180	1.06876	1.05387	0.96878
	3.0	0.0	-3.84900	-2.87641	-2.09447	-2.53480	-13.028885	-29.60628
		2.0	-22.64288	-19.22132	-14.07139	-11.30301	-6.98149	-9.63358
		5.0	-102.26139	-96.45985	-86.35808	-79.65398	-57.76860	-44.12336
3.0	-3.0	0.0	7.67246	6.45388	5.47794	6.02703	19.15162	42.86510
		2.0	38.65912	33.42891	24.76895	19.69807	9.88495	12.51908
		5.0	158.42317	147.57876	128.33798	115.61782	75.66300	52.77385
	0.0	0.0	0.65175	0.66865	0.68187	0.67447	0.46948	8.01E-002
		2.0	0.65248	0.68827	0.73245	0.74715	0.68716	0.49473
		5.0	0.82766	0.86500	0.91572	0.93891	0.95093	0.88927
	3.0	0.0	-6.36896	-5.11658	-4.11419	-4.67809	-18.21264	-42.70484
		2.0	-37.35414	-32.05236	-23.30403	-18.20377	-8.51062	-11.52960
		5.0	-156.76783	-145.84876	-126.50653	-113.73999	-73.76112	-50.99529

Table 6: Heat transfer parameter $-\theta'(0)$ is tabulated at some chosen rotation numbers, $\omega = 0.0, 2.0, 5.0$, radial electric parameters, $\gamma = -0.6, -0.4, 0.0, 0.3, 1.5, 2.5$, for the two different Magnetic interaction numbers $M_n = 1.0, 3.0$, and Eckert numbers $E_c = -3.0, 0.0, 3.0$ respectively, and fixed Prandtl number $P_r = 1.0$ over stretchable disk.

4. CONCLUSIONS

In this work, effects of radial electric field in steady-incompressible boundary layer flow over a shrinking/stretching disk have been investigated. Navier-stokes equations, energy equation and Maxwell equation were reconstructed using self-consistent assumptions. The resulting system has been solved numerically by using Chebyshev collocation method. Behavior of the velocity and temperature profiles in this system are obtained and displayed graphically.

Therefore, influences of radial electric parameter, Eckert parameter, magnetic interaction parameter and rotation parameter are observed from given graphs and tables. One of the main outcomes of the present study is that negative radial electric parameter has a big effect on temperature profiles both in shrinking and stretching disk. It can be concluded from figures (8-11) and tables (5-6) that number of presence of temperature profiles increases for the negative radial electric parameters as rotation parameter increases in both shrinking and stretching disks.

REFERENCES

[1] Altan T., Oh S. and Gerel H. *Metal forming Fundamentals and Applications*, American Society of Metals, Metals Park, 1979.

[2] Backok N., Ishak A., Pop I. *Unsteady boundary-layer flow and heat transfer of a nanofluid over a permeable stretching/shrinking sheet*. Int. J. Heat Mass Transfer, 55, 2102-2109, 2012.

[3] Benton E. T., *On the flow due do rotating disk*. Journal of Fluid Mechanics, 24, 781-800, 1966.

[4] Cochran W. G., *The flow due to rotating disk*. Proceeding of the Cambridge Philosophical Society, 30, 365-375, 1934.

[5] Cortell R., *On a certain boundary value problem arising in shrinking sheet flows*, Appl. Math. Comput., 217, 4086-4093, 2010.

[6] Crane L., J., *Flow past a stretching plate*, Z. Angew. Math. Phys. 21, 645-647, 1970.

[7] Evans H. L., *Laminar Boundary Layer Theory*. Addison-Wesley, 1968.

[8] Fang T., *Flow over a stretchable disk*. Phys. Fluids bf 19 ,128105, 2007.

- [9] Fang T., Zhang J., *Thermal boundary layers over a shrinking sheet: an analytical solution*. Acta Mech., 209, 325-343, 2010.
- [10] Fang T., Lee C. F. F. & Zhang J. *The boundary layers of an unsteady incompressible stagnation-point flow with mass transfer*. Int. J. Nonlinear Mech. ,46(7), 942-948, 2011.
- [11] Fisher E. G., *Extrusion of Plastics*, Wiley, New York, 1976.
- [12] Hossain, M. A.; Hossain, A.; Wilson, M., *Unsteady flow of viscous incompressible fluid with temperature-dependent viscosity due to a rotating disk in the presence of transverse magnetic field and heat transfer*. International Journal of Thermal Sciences, 40, 11-20, 2001.
- [13] Karman, T. V., *Über laminare und turbulente Reibung*. Zeitschrift für angewandte Mathematik und Mechanik. 1, 233-252, 1921.
- [14] Khan Y., Wu Q., Faraz N., Yildirim A., *The effects of variable viscosity and thermal conductivity on a thin film flow over a shrinking/stretching sheet* Comput. Math. Appl., 61, 3391-3399, 2011.
- [15] Makukula Z. G., Sibanda P., Motsa S. S., Shateyi S., *On new numerical techniques for the MHD flow past a shrinking sheet with heat and mass transfer in the presence of a chemical reaction* Math. Probl. Eng., 2011, 1-19, 2011.
- [16] Miklavcic M., Wang C. Y., *Viscous flow due to a shrinking sheet* Q. Appl. Math., 64, 283-290, 2006.
- [17] Schlichting H., *Boundary Layer Theory* McGraw-Hill, New York, 1968.
- [18] Sparrow E. M., Cess, R. D. *Magnetohydrodynamic flow and heat transfer about a rotating disk*. Trans. ASME Ser. E. J. Appl. Mech. 29, 181-192, 1962.
- [19] Tadmor Z, Klein I. *Engineering principles of plasticating extrusion*, Polymer Science and Engineering Series, New York, Van Nostrand Reinhold, 1970.
- [20] Turkyilmazoglu M., *Effects of uniform radial electric field on the MHD heat and fluid flow due to a rotating disk*. Internat. J. Engrg. Sci. 51, 233-240, 2012.
- [21] Turkyilmazoglu M., *A class of exact solutions for the incompressible viscous magnetohydrodynamic flow over a porous rotating disk*. Acta Mech. Sin. 28, bf 2, 335-347, 2012.
- [22] Turkyilmazoglu M., *MHD fluid flow and heat transfer due to a stretching rotating disk*. Int. J. Therm. Sci. 51, 195-201, 2012.
- [23] Turkyilmazoglu M., *MHD fluid flow and heat transfer due to a shrinking rotating disk*. Computers & Fluids, 90, 51-56, 2014.
- [24] Uygun N., *Effect of Hall current on the MHD Fluid Flow and Heat Transfer due to a rotating disk with uniform radial electric field*. HJMS 46(6), 1445-1462, 2015.
- [25] Wang C. Y., *The three-dimensional flow due to a stretching at surface*. Phys. Fluids 27, 1915, 1984.
- [26] Wang C. Y., *Exact solutions of the unsteady Navier-Stokes equations*. Appl. Mech. Rev. 42, S269, 1989.
- [27] Wang C. Y., *Exact solutions of the steady state Navier-Stokes equations*. Annu. Rev. Fluid Mech. 23, 159, 1991.
- [28] Wang C. Y., *Stagnation flow towards a shrinking sheet* Int J Non-linear Mech, 43, 377-382, 2008.
- [29] Watson L. T., Wang C. Y., *Deceleration of a rotating disk in a viscous fluid*. Phys Fluids 22(12), 2267-2269, 1979.